PROBABILISTIC ANALYSES OF LANDSLIDE TSUNAMI HAZARDS

Philip Watts

Applied Fluids Engineering, Inc., PMB #237, 5710 E. 7th Street, Long Beach, CA, 90803, U.S.A.
E-mail: **phil.watts@appliedfluids.com**

ABSTRACT

A review of tsunamis during the 1990s reveals that around 30% of maximum runup peaks probably involved tsunamigenic mass failure. Submarine mass failure includes underwater slides, underwater slumps, and reef failure, most often triggered by a nearby earthquake. Earthquakes above magnitude 7 are typically accompanied by thousands of mass failure events, although most of these will not be tsunamigenic. A geological context derived from marine surveys is needed to identify prospective mass failures and to predict their size and location. Probabilistic calculations of underwater slides and slumps throughout the Pacific Basin can yield preliminary probability distributions of mass failure generated tsunamis. Tsunami amplitude is estimated from accurate curve fits based on numerical simulations of mass failure events. As observed, about 35% of all earthquakes generate landslide tsunamis that surpass coseismic displacement in amplitude. A finite probability exists for mass failure to generate tsunamis with amplitudes in excess of 10 meters. The probabilities of nearshore and offshore earthquakes can be converted directly into tsunami hazards from submarine mass failure. Indicators of prospective tsunamigenic landslides such as sediment shear strength improve our ability to predict future events and to assess their impact on coastal populations and development. This kind of probabilistic calculation may play an important role in tsunami risk assessment from landslide tsunamis.

1. INTRODUCTION

Increased human coastal population and development coupled with devastating losses in recent history motivate tsunami hazard assessment efforts. Tsunamis may be generated by volcanic eruptions, coseismic sea floor displacement, gas hydrate phase change, underwater landslides, and oceanic meteor strikes. Landslide tsunamis remain one of the least studied of these five mechanisms, in part because their occurrence is concealed and in part because of the complicated dynamics involved in failure, center of mass motion, and landslide deformation [Watts, 2001]. Scientists are currently unable to assess some underwater landslide hazards, to predict their occurrence following a nearby earthquake, and to evaluate their tsunamigenic potential. In this paper, we will outline a technique that predicts the probability of tsunamigenic mass failures.

1.1 REVIEW OF RECENT TSUNAMIS

Historical records verify the tsunami hazards posed by submarine mass failure. Most damage and fatalities during or following the 1964 Good Friday, Alaskan Earthquake resulted from local waves generated by submarine mass failure [Plafker *et al*., 1969]. Since 1992, there have been at least twelve major local tsunamis. The majority of these tsunamis demonstrated regions of peaked longshore runup distribution. For example, runup produced by the Flores Island tsunami showed a modest runup plateau of 8 m punctuated by numerous large peaks up to 26 m in amplitude that correlated with reef failures and subaerial landslides [Imamura and Gica, 1996]. The 1998 Papua New Guinea tsunami has been the subject of extensive marine surveys to describe the slump source and to model the tsunami generation, propagation, and inundation [Tappin *et al*., 1999, 2001, 2002]. Five other events, Nicaragua, Mindoro, Skagway, Kamchatka, and Izmit Bay are known or suspected to have involved significant

landslide tsunami generation, with or without significant coseismic displacement. Throughout the Pacific, tsunami amplitude and earthquake magnitude records acquired during the 1990s suggest that submarine mass failures generate the maximum tsunami amplitude in around 30% of events [Watts, 2002].

2. TYPES OF SUBMARINE MASS FAILURE

Damaging tsunamis may result from the failure of sediment along steep fjords banks, near boundaries of submarine canyon systems, at active river deltas, along volcanic islands or ridges, or at submerged alluvial plains including continental margins [Hampton *et al.*, 1996]. Underwater landslides or mass failures include slides and slumps as two distinct end members of a continuous spectrum of submarine mass failure [Prior and Coleman, 1979; Edgers and Karlsrud, 1982; Schwab *et al.*, 1993]. Underwater slides are identified by translational failure, while underwater slumps are defined to undergo rotational failure [Schwab *et al.*, 1993]. Terzaghi [1956] showed that underwater slides and slumps can often be related to excess pore water pressures. Prior and Coleman [1979] attribute excess pore water pressure to low tides, artesian water flows, recent external loads, rapid sedimentation, seismic ground motions, construction induced vibrations, volcanic activity, vaporization of gas hydrates, wave action, or any combination of these or similar factors. Most tsunamigenic underwater slides and slumps are triggered by local earthquakes, but not all [Bjerrum, 1971].

2.1 CENTER OF MASS MOTIONS

Water wave amplitudes above an underwater slide or slump scale with characteristics of center of mass motion [Watts, 1998, 2000]. We contrast the center of mass motions of submarine slides and slumps by the dominant retardive force, providing convenient asymptotic limits for these two types of motion. Many real failure events are expected to move in a manner combining aspects of each analysis. As such, these results provide end members for landslide center of mass motions. Center of mass motion is parametrized by the characteristic time of motion t_o and the characteristic distance of motion s_o, where the landslide initial acceleration $a_o=s_o/t_o^2$ governs tsunami generation. These quantities are ultimately dependent on the sediment type and density as well as the landslide shape [Watts, 1998].

3. PROBABILISTIC MODEL DESCRIPTION

A predictive model is developed to examine the probability distribution of tsunami amplitudes generated by submarine mass failure. The model uses realistic uniform or Poisson probability distributions to span the complete parameter space of nearshore geology within the Pacific Basin. We ask the following question: What parameters along the presumed failure plane govern or dominate tsunamigenic landslides? To answer this question, we treat each model parameter a random quantity in what is effectively a Monte-Carlo scheme. That is, each parameter is fixed in value for each random realization of all parameters along the failure plane. The dependence and sensitivity of tsunami amplitude with respect to each random parameter is then evaluated. The model is divided into three sections: earthquake engineering characteristics, sediment stability calculations, and tsunami amplitude estimates. More model details and equations can be found in Watts [2002].

3.1 EARTHQUAKE ENGINEERING

Kramer [1996] provides correlations for peak horizontal acceleration and frequency of ground motion with respect to earthquake moment magnitude. This work enables one to characterize ground motion during a given earthquake. Our algorithm begins by choosing a random earthquake magnitude in the range expected off a given margin. The distance of the earthquake epicenter from the continental shelf is chosen at random from within a reasonable range of influence that depends on moment magnitude. The depth d at the middle of potential mass failure is then chosen at random subject to several geometric constraints based on typical bathymetry. This depth is the first descriptor of mass failure geometry. The peak horizontal acceleration, frequency of oscillation, and number of cycles are then calculated from earthquake engineering correlations [Kramer, 1996].

3.2 SEDIMENT STABILITY CALCULATIONS

Typical sediment characteristics and sedimentation rates are needed to model sediment response to a nearby earthquake. Earthquake and sediment parameters become inputs in the sediment failure calculations [Morgenstern and Price, 1965; Turner and Schuster, 1996]. Several different failure modes are possible for any given sediment. We did not consider the effects of sediment grain size distribution, variations and changes in sediment type, seismic and landslide histories, overconsolidation, liquefaction, or storm waves in our current calculations. For now, quasi-static stability analysis is employed because of its relative simplicity. We assume a bulk sediment density of ρ_b=1900 kg/m^3 throughout this work. Our algorithm randomly chooses a mean yearly sedimentation rate and a reasonable slope inclination. This slope is the second descriptor of mass failure geometry.

The algorithm then splits into sandy/silty sediments and clayey sediments with equal probability [Schwab *et al.*, 1993]. The algorithm chooses a random friction angle, cohesion, and pore water diffusivity suitable for sands and silts. For clays, the algorithm chooses random plasticity and liquidity indices and then calculates shear strength and pore water diffusivity from standard correlations [Bardet, 1997]. For both sediment types, sediment is built up based on an instantaneous sedimentation load followed by pore water diffusion for the rest of that year. This enables pore water pressure to accumulate and contribute to failure. Failure occurs when the computed depth of failure matches the current depth of accumulated sediment. We assume that a sufficiently thick sediment blanket exists to accommodate such failure thicknesses. The algorithm randomly chooses the mass failure length and width according to the sediment type and available failure scarce data [Prior and Coleman, 1979; Schwab *et al.*, 1993]. The mass failure thickness, length, and width complete the description of mass failure geometry. The five geometric variables suffice to calculate the characteristic tsunami amplitude [Grilli and Watts, 1999; Goldfinger *et al.*, 2000; Grilli *et al.*, 2002].

3.3 TSUNAMI AMPLITUDE ESTIMATES

In this work, we employ the model problem whereby an underwater slide or slump is modeled as a semi-ellipse resting on a straight incline with angle θ from horizontal [Grilli and Watts, 1999]. We consider the semi-ellipse as a good approximation of most underwater slide and slump shapes. The semi-ellipses have a maximum thickness T along half of the minor axis that is perpendicular to a major axis of total length b [Grilli and Watts, 1999]. The semi-ellipse has an initial vertical submergence d at the middle of the landslide and a width w running along the slope. We prescribe either slide or slump center of mass motion along the

incline and assume negligible deformation. Numerical experiments have been reduced to predictive curve fits of tsunami amplitude that are simple analytical functions of nondimensional quantities [Grilli and Watts, 1999; Goldfinger *et al.*, 2000; Grilli *et al.*, 2002]. Such curve fits provide a rapid and inexpensive means to estimate tsunami amplitude and gauge the sensitivity of that amplitude to landslide characteristics. Each mass failure shape or motion has a separate tsunami amplitude equation, so there is an equation for underwater slides and a separate equation for underwater slumps. The maximum tsunami amplitude above the initial mass failure location is chosen here as a characteristic tsunami amplitude [Watts, 1998, 2000].

3.4 LIMITATIONS AND CONSTRAINTS

Our analyses of slope stability assume an infinite slope as well as yearly deposition of a uniform sediment. These approximations arise because we assume complete knowledge of the model parameters along the failure plane without attempting to track the long term evolution of the continental slope itself. Because we study a single mass failure per earthquake, our results apply to the worst case failure or largest possible landslide tsunami. We have attempted to use uniform probability distributions whenever possible given the general nature of this study. Site specific model runs would use much more refined probability distributions. Therefore, the results given here are general and subject to revision should a specific site be chosen for careful study.

4. PROBABILISTIC MODEL RESULTS

In general, it is possible to have coseismic displacement tsunami generation without mass failure, and mass failure tsunami generation without significant coseismic displacement [Watts, 2001]. Consequently, we focus on the landslide tsunami results in our presentation, with the understanding that significant coseismic displacment may also occur. Fig. 1 refutes a commonly held assumptions regarding landslide tsunamis. Large tsunamis can be generated with roughly equal probability by earthquakes with moment magnitudes ranging from 5-7. This result is not substantially modified if one considers peak horizontal acceleration as the independent parameter. Landslide tsunami amplitude is largely independent of earthquake magnitude. Almost all of the random parameters produced plots similar to this one for both slides and slumps.

Fig. 2, involving only clay simulations, shows that tsunamigenic mass failure occurs in regions of high sediment strength. A low liquidity index is indicative of stiff clay with significant shear strength [Bardet, 1997]. Mass failure is more probable in sediments with low strength, although mass failure tends to be shallow and not tsunamigenic. River deltas offer a case in point for many thin mass failures [Terzaghi, 1956]. Cores taken off Papua New Guinea in the source region of the 1998 tsunami source revealed stiff clay with presumably strong shear strength [Tappin *et al.*, 2001, 2002]. Given the apparent combination of stiff clays near a region of strong ground motion, a catastrophic tsunami generated by a large submarine mass failure fits with these probabilistic results. We have analyzed the sensitivity of tsunami amplitude to all earthquake and sediment parameters elsewhere [Watts, 2002].

4.1 FREQUENCY OF LANDSLIDE TSUNAMIS

We find that earthquakes fail to generate any failure in clayey sediments 20% of the time and in sandy/silty sediments 50% of the time, neglecting liquefaction as a failure mechanism.

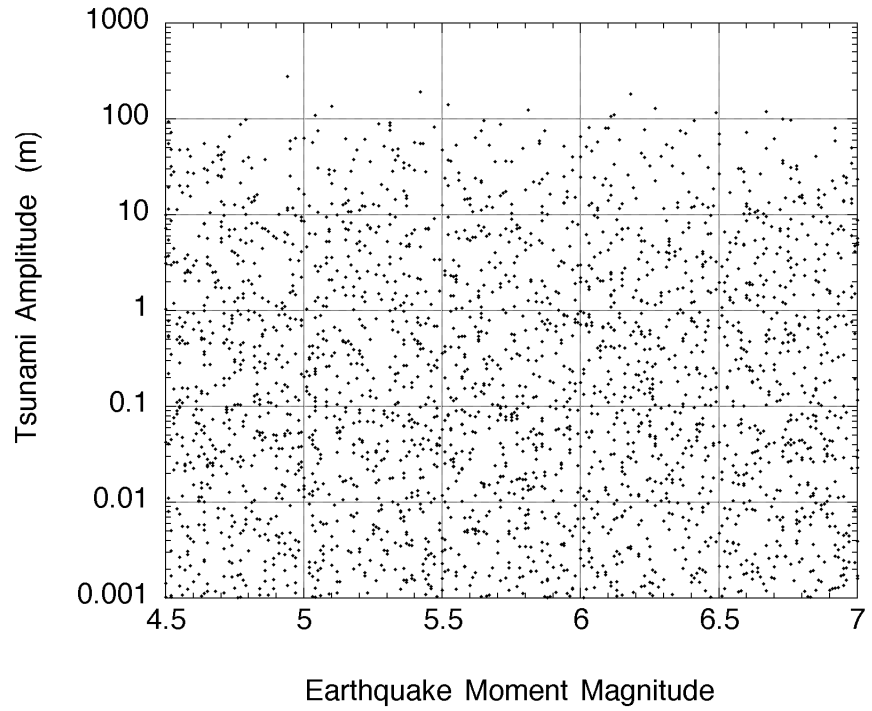

Figure 1. Characteristic tsunami amplitude versus earthquake moment magnitude.

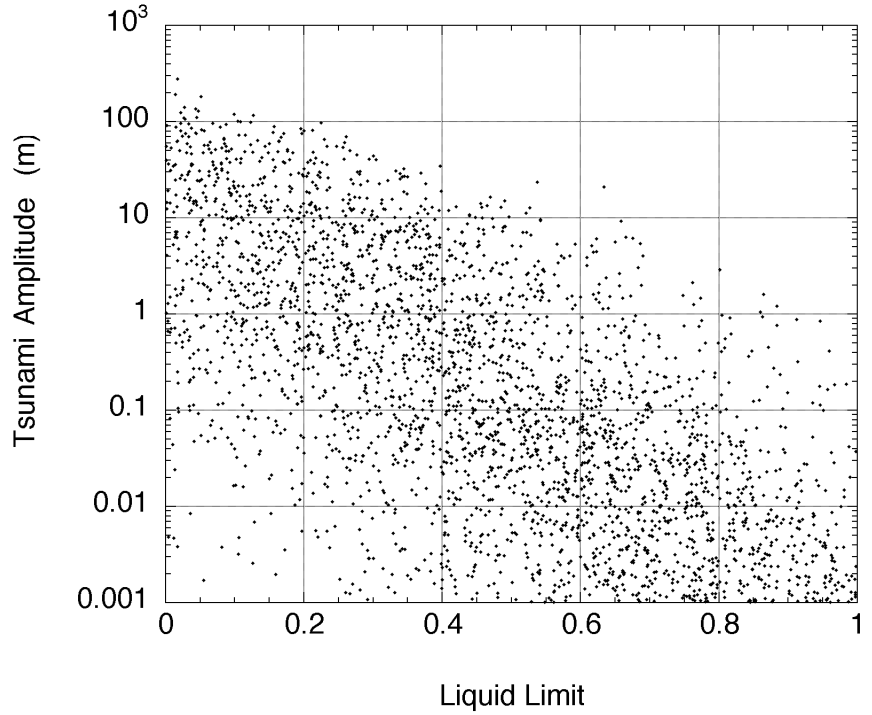

Figure 2 Characteristic tsunami amplitude versus liquid limit.

Landslide tsunamis greater than 1 cm should be generated by approximately 47% of all earthquakes. In agreement with observations, we find that 36% of landslide tsunamis surpass an estimate of the vertical coseismic displacement of the earthquake that triggered failure.

5. CONCLUSIONS

We present a probabilistic estimate of tsunami hazards from submarine mass failures. The tsunami amplitude curve fits used herein enable rapid case studies and tsunami hazard assessment. In particular, we show that peaks in tsunami amplitude such as the 26 m wave that devastated Riangkroko, Indonesia in 1992 could have been expected from local tsunamigenic landslides. Throughout the Pacific Basin, the potential exists to generate local tsunami amplitudes in excess of 10 m, although further study is needed to identify specific sites and to assess the probabilities of any such events. To that end, several random parameters have been shown to significantly influence tsunamigenic landsliding: mean sedimentation rate W for sandy or silty slopes, and liquid limit LL for clayey slopes. Other parameters studied here may strongly influence the morphology and evolution of a margin even if they do not correlate with tsunami amplitude. The ensemble of landslide tsunamis produced in this study seems to capture some general features of the ensemble of landslide tsunamis observed throughout the Pacific Basin during the 1990s. Despite these promising results, we cannot claim that we have reproduced the correct probability distribution for landslide tsunamis because a greater variety of constitutive relations and failure mechanisms and probability distributions needs to be considered for the sake of completeness. For any site specific study, the parameter ranges would need to be significantly reduced.

ACKNOWLEDGMENTS

The author wishes to thank Prof. Jean-Pierre Bardet for numerous fruitful discussions, and Jose Borrero for help programming some equations into the computer program.

REFERENCES

Bardet J.-P., 1997: Experimental soil mechanics. Prentice Hall, Upper Saddle River, NJ.

Bjerrum L., 1971: Subaqueous slope failures in Norwegian fjords. *Nor. Geotech. Inst. Bull.*, 88, 1-8.

Edgers L., and Karlsrud K., 1982: Soil flows generated by submarine slides: Case studies and consequences. *Nor. Geotech. Inst. Bull.*, 143, 1-11.

Goldfinger C., Kulm L. D., McNeill L. C., Watts P., 2000: Super-scale failure of the Southern Oregon Cascadia Margin. *PAGEOPH*, 157, 1189-1226.

Grilli S. T., and Watts P., 1999: Modeling of waves generated by a moving submerged body: Applications to underwater landslides. *Engrg. Analysis with Boundary Elements*, **23**(8), 645-656.

Grilli S. T., Vogelmann S., and Watts P., 2002: Development of a 3D numerical wave tank for modeling tsunami generation by underwater landslides. *Engrg. Analysis with Boundary Elements*, **26**(4), 301-313.

Hampton M. A., Lee H. J., and Locat J., 1996: Submarine landslides. *Rev. Geophys.*, **34**(1), 33-59.

Imamura F., and Gica E. C., 1996: Numerical model for tsunami generation due to subaqueous landslide along a coast. *Sci. Tsunami Hazards*, 14, 13-28.

Kramer S. L., 1996: *Geotechnical earthquake engineering*. Prentice Hall, Upper Saddle River, NJ.

Morgenstern N. R., and Price V. E., 1965: The analysis of the stability of general slip surfaces. *Geotechnique*, 15, 79-93.

Plafker G., Kachadoorian R., Eckel E. B., and Mayo L. R., 1969: The Alaska earthquake March 27, 1964: Various communities. U.S. Geol. Surv. Prof. Paper 542-G, U.S., Dept. of Interior, Washington, D.C.

Prior D. B., and Coleman J. M., 1979: Submarine landslides: Geometry and nomenclature. *Z. Geomorph. N. F.*, **23**(4), 415-426.

Schwab W. C., Lee H. J., and Twichell D. C., 1993: Submarine landslides: Selected studies in the U.S. exclusive economic zone. U.S. Geol. Surv. Bull. 2002, U.S., Dept. of Interior, Washington, D.C.

Tappin D. R., Matsumoto T., and shipboard scientists., 1999: Offshore geological investigation of the July 1998 Sissano tsunami, Papua New Guinea. *EOS, Trans. Am. Geophys. Union*, **80**(30), 329.

Tappin D. R., Watts P., McMurtry G. M., Lafoy Y., and Matsumoto T., 2001: The Sissano, Papua New Guinea Tsunami of July 1998 -- Offshore Evidence on the Source Mechanism. *Marine Geology*, 175, 1-23.

Tappin D. R., Watts P., McMurtry G. M., Lafoy Y., and Matsumoto T., 2002: Prediction of slump generated tsunamis: The July 17 th 1998 Papua New Guinea event. *Sci. Tsunami Hazards*, **20**(4), 222-238.

Terzaghi K., 1956: Varieties of submarine slope failures. *Proc. 8th Texas Conf. Soil Mech. Found. Eng.*, 1-41.

Turner A. K., and Schuster R. L., 1996: *Landslides: Investigation and mitigation*. Special Report 247, Trans. Res. Board, National Academy Press, Washington, D.C.

Watts P., 1998: Wavemaker curves for tsunamis generated by underwater landslides. *J. Wtrwy, Port, Coast, and Oc. Engrg.*, ASCE, **124**(3), 127-137.

Watts P., 2000: Tsunami features of solid block underwater landslides. *J. Wtrwy, Port, Coast, and Oc. Engrg.*, ASCE, 126(3), 144-152.

Watts P., 2001: Some opportunities of the landslide tsunami hypothesis. *Sci. Tsunami Hazards*, **19**(3), 126-149.

Watts P., 2002: Probabilistic predictions of landslide tsunamis off Southern California. *Natural Hazards*, accepted.